JETIR.ORG ISSN: 2349-5162 | ESTD Year : 2014 | Monthly Issue

JOURNAL OF EMERGING TECHNOLOGIES AND INNOVATIVE RESEARCH (JETIR)

An International Scholarly Open Access, Peer-reviewed, Refereed Journal

An Exploration towards the Integrative MATLAB-Based Computational Modelling for Advanced Failure Analysis and Structural Optimization of Gas Turbine Blades

[1] Kaushal Kishor, [2] Anjani Kumar Singh

[1] Department of Mechanical Engineering, School of Engineering & Technology, YBN University, Ranchi, Jharkhand

[2] Department of Mechanical Engineering, School of Engineering & Technology, YBN University, Ranchi, Jharkhand

Abstract: This research presents the development and implementation of predictive computational models for failure analysis in turbine blades of high-performance gas turbine engines. By integrating classical analytical methods with advanced computational techniques using MATLAB, the study simulates the complex mechanical behaviour of turbine blades under extreme thermal, aerodynamic, and centrifugal forces. The methodology encompasses finite element analysis, fatigue life estimation via Basquin's equation, and machine learning approaches to predict potential failure points and optimize design parameters. Results from MATLAB simulations and GUI-based analyses demonstrate significant correlations between blade geometry, operating conditions, and failure risks, providing a robust framework for proactive maintenance and design enhancements in turbine technology.

Keywords: Predictive Modelling, Failure Analysis, Turbine Blades, Gas Turbine Engines, MATLAB Simulation, Fatigue Life Estimation.

1. INTRODUCTION

The demand for high-performance gas turbines has escalated in recent decades, driven by advancements in aerospace and power generation technologies (Choi & Lee, 2010; Frunzăverde et al., 2010). These engines must operate efficiently at higher temperatures and speeds while maintaining reliability and longevity, making turbine blades—subjected to extreme thermal and mechanical conditions—pivotal to overall performance (Silveira et al., 2010). Predicting blade failure is crucial for safety and cost-effectiveness (Barella et al., 2011), motivating the development of predictive computational models aimed at mitigating the risks associated with premature failure (Qu et al., 2013). In gas turbines, blades experience complex mechanical stresses centrifugal forces from high rotation, aerodynamic forces from hot gas flow, and thermal stresses due to rapid temperature fluctuations (Chen & Kam, 2011). Understanding these stress interactions is vital for designing durable components (Kargarnejad & Djavanroodi, 2012). Traditional testing methods, while informative, can be expensive, time-consuming, and carry safety concerns (Rao, Kumar, & Prasad, 2014). Through contrast, predictive modelling offers a virtual testbed to simulate real-world conditions and evaluate performance without extensive physical prototyping (Poursaeidi et al., 2013). Techniques such as Finite Element Analysis (FEA) have thus become integral in assessing blade integrity under various stresses. Developing predictive models for turbine blade failure requires integrating material properties, mechanical loads, and environmental factors (Yang & Sun, 2013). High-performance blades, often fashioned from nickel-based superalloys, are remarkably strong at elevated temperatures yet still prone to fatigue, creep, and thermal fatigue (Lee et al., 2012). Accounting for each failure mechanism demands a unified approach that combines classical analytical methods with advanced computational techniques.

MATLAB's specialized toolboxes and robust numerical solvers facilitate this integration, enabling detailed simulations of turbine blade behaviour under operational extremes.

Through MATLAB-based FEA, fatigue analyses, and optimization algorithms, engineers can accurately predict blade responses, identify probable failure points, and propose design or material modifications (Silveira et

al., 2010). Additionally, machine learning models such as neural networks can be trained on simulation data to produce probabilistic failure estimates, supporting proactive maintenance and repair strategies (Yang & Sun, 2013). The result is a more thorough and cost-effective approach to turbine blade design. Predictive computational models also allow engineers to explore a wide range of design scenarios, material choices, and operating conditions before finalizing a solution. Such flexibility leads to improved optimization for specific applications, enhancing blade durability and efficiency (Rao et al., 2014). Moreover, the ability to forecast failures before they occur supports proactive maintenance, reducing overall lifecycle costs and increasing operational safety (Kargarnejad & Djavanroodi, 2012). Through embedding these models into the design, testing, and maintenance processes, the aerospace and power generation industries can drive continuous innovation in turbine technology while minimizing risks tied to blade failure (Qu et al., 2013).

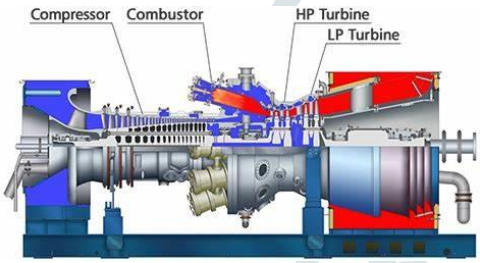

Fig. 1. H-100 Gas Turbines

Source:
https://power.mhi.com/products/gasturbines/lineup/h100/

The gas turbine operates through four main stages: intake, compression, combustion, and exhaust. Air enters through the intake and is compressed to high pressure in the compressor. This compressed air is mixed with fuel and ignited in the combustor, generating high-temperature, high-pressure gases. These gases expand through the high-pressure (HP) and low-pressure (LP) turbines, producing rotational energy that drives the compressor and an external load, such as a generator or propulsion system. The remaining energy is expelled through the exhaust, creating thrust or additional power. This efficient energy conversion process is widely used in aerospace and power generation applications.

1.1 The Growing Demand for High-Performance Gas Turbines

The global demand for high-performance gas turbines has surged due to several factors, including rapid advancements in aerospace, energy production, and military technologies. Gas turbines, which are the heart of many modern propulsion and power systems, need to operate efficiently under extreme conditions. High temperatures, high rotational speeds, and high mechanical loads are standard challenges that these turbines face in their operational environments. In industries such as aerospace and power generation, the ability to achieve higher efficiency and reliability while withstanding these challenging operational environments is becoming increasingly important (Clarkson et al., 2016).

In aerospace applications, for instance, the demand for more fuel-efficient engines drives the need for turbines capable of enduring high temperatures and delivering maximum power with minimum weight. The aviation industry, particularly, relies on gas turbines to deliver thrust at the lowest possible weight while optimizing fuel efficiency. Similarly, in the power generation sector, gas turbines are often used in combined-cycle power plants, where their efficiency can determine the economic feasibility of electricity generation, especially with rising global demand for sustainable energy.

1.2 The Role of Gas Turbines in Aerospace and Power Generation

Gas turbines are widely used in aerospace propulsion systems, such as jet engines, and power generation systems, including electricity-producing plants. In aerospace, turbine engines like turbojets, turbofans, and turboprops provide thrust for aircraft propulsion. The technological advancements in material science and computational engineering have allowed turbines to achieve significant performance gains, but these systems are often operating at the edge of their mechanical limits due to the demanding operational conditions they face.

In power generation, gas turbines play a critical role in both standalone plants and combined-cycle systems. Combined-cycle plants use the exhaust heat from the gas turbines to produce steam, which powers a steam turbine, further increasing efficiency. These turbines are required to operate reliably over long periods, making reliability and longevity critical for economic feasibility in power production (Zhao et al., 2015).

1.3 Centrifugal Forces and Their Impact on Turbine Blade Mechanics

1.3.1 The Nature of Centrifugal Forces

Centrifugal forces are generated due to the rotational motion of the turbine blades. As the turbine spins at high rotational speeds, the blades are subject to a centrifugal force that acts outward from the centre of rotation. The magnitude of this force increases with the speed of rotation and the mass of the blades. In high-performance gas turbines, blades can reach rotational speeds of up to 15,000 revolutions per minute (RPM), making centrifugal forces a significant factor in turbine blade mechanics.

The centrifugal force Fc on a turbine blade equals its mass m multiplied by the square of the angular velocity ω2 and by the distance from the centre of rotation r. In other words:

$$\text{Centrifugal Force} = \text{Mass} \times (\text{Angular Velocity})^2 \times \text{Radius}$$

$$Fc = m.\ \omega^2.\ r$$

This force acts to pull the turbine blades outward, creating tensile stresses along the length of the blade. As a result, the blade material is subjected to stretching, and the centrifugal force can cause permanent deformation if the blade is not properly designed (Khawaja & Moatamedi, 2014).

2. REVIEW OF LITERATURE

In this Section, the fundamental concepts and overarching objectives of this research were presented, underlining the critical importance of reliable, high-performance turbine blades in gas turbine engines. We introduced the motivation behind developing predictive computational models namely, to anticipate potential failure points and enhance overall efficiency under extreme operating conditions. The discussion highlighted the need for integrative approaches that combine thermodynamic analysis with robust material and structural assessments.

Frunzăverde et al. (2010) investigated a failed Francis turbine blade after in-situ welding, attributing fatigue failure to welding seam defects. Hydrogen embrittlement further accelerated the process, highlighting the need for precise repair methods.

Silveira, Atxaga, and Irisarri (2010) analyzed aircraft blade failures, linking one case to foreign object debris and another to thermo-mechanical fatigue. Microstructural defects worsened the damage, affecting turbine performance.

Choi and Lee (2010) examined a gas turbine blade failure during start-up, caused by fatigue due to transient combustion events. Resonance conditions amplified stresses, leading to fracture.

Sujata et al. (2010) studied gas turbine blade failures due to creep and stress rupture, emphasizing microstructural deterioration. Their analysis helped improve turbine maintenance strategies.

Shankar, Kumar, and Prasad (2010) assessed blade disc integrity, considering material uncertainties and temperature effects. Their findings emphasized accurate design methodologies to minimize fatigue failures.

Barella et al. (2011) investigated a third-stage turbine blade failure in a thermal power plant, attributing high-cycle fatigue to fretting. Their study provided insights for improving turbine reliability.

Adamou et al. (2023) explored AM-enabled combustion chambers, improving efficiency and emissions control in microcomputer gas turbines.

Alnaeli et al. (2023) emphasized material selection in turbine combustors, addressing thermal deterioration and mechanical failures for alternative fuels.

Hong and Kim (2023) developed a CNN-RNN model for gas turbine performance prediction, enhancing maintenance and efficiency.

Zhang et al. (2024) proposed a universal instability warning logic, improving gas turbine reliability and safety.

Jin et al. (2024) studied flame stability in reverse-flow combustors, offering insights for compact combustor designs.

Asaad, Shaker, and Kdhim (2024) analyzed turbine blade materials and designs to enhance durability and performance.

Enyia et al. (2024) examined the impact of an afterburner on gas turbine efficiency, boosting power output for Nigeria's energy needs.

Feiz et al. (2024) investigated additive manufacturing for fuel nozzles, optimizing combustion efficiency and emission control.

3. RESEARCH METHODOLOGY

These user inputs define the primary geometric and operating parameters for the turbine. The number of blades (B) influences torque and aerodynamic performance, while the rotor radius (R) determines the total swept area. The hub radius (r_h) defines the inner boundary for the blades, affecting effective blade length. Air density (ρ) is crucial for estimating aerodynamic forces, as it dictates available kinetic energy. The design wind speed (V_design) is the reference flow velocity for optimal performance. Finally, the tip-speed ratio (λ) guides the rotor's rotational speed relative to the incoming flow, balancing efficiency and structural constraints. Effective design ensures reliability.

The second step involves **radial discretization**, where the blade span from the hub radius rh to the outer radius RRR is divided into N segments. These radial positions, labelled ri, are generated in MATLAB using the Lin space function, creating a uniformly spaced vector from rh to R. Each segment represents a discrete cross-section of the blade, enabling localized aerodynamic calculations.

The third step focuses on **chord and twist** computations, crucial for ensuring optimal aerodynamic performance. First, the **local tip-speed ratio** is determined at each radial position as

$$\text{Local TSR (ri)} = \omega Ti / V_{design}$$

then subtracting the design angle of attack α_{design}.

Power Calculations

The power estimates are based on the formula:

$$P = 1/2\ \rho A V^3 Cp$$

where:

- P is the power,
- ρ is the air density,
- $A=\pi R^2$ is the swept area of the rotor,
- V is the design wind speed,
- Cp is the power coefficient.

3.1 Algorithm Design

Step 1: Define the Problem

Clearly articulate the problem to be solved, including the input, output, and constraints. This helps ensure that the algorithm's purpose is well understood before beginning the design process. For instance, in the circumstance of a high-pressure gas turbine engine (HPGTE) simulation, the problem could involve calculating stage-by-stage thermodynamic parameters.

Step 2: Analyze the Problem
Break down the problem into smaller, manageable components. Identify dependencies, constraints, and edge cases that the algorithm must handle. For instance, in the HPGTE simulation, analyse processes like compression, combustion, and turbine operation individually.

Step 3: Identify Inputs and Outputs
List all the inputs required for the algorithm and define the desired outputs. In the HPGTE example, inputs might include mass flow rate, pressure ratios, and efficiency values, while outputs could include temperature, pressure, and work done at each stage.

Step 4: Select an Approach
Choose an appropriate approach for solving the problem. This might involve selecting a numerical method, iterative process, or optimization technique. For example, thermodynamic processes might use equations for isentropic efficiency or conservation of energy.

Step 5: Develop a High-Level Plan
Create a high-level overview of the algorithm. Divide the solution into sequential steps or modules, ensuring logical flow and completeness. For HPGTE, this could involve designing functions for the compressor, combustor, turbine, and exhaust stages.

Step 6: Write Pseudocode
Draft pseudocode that outlines the algorithm's logic in a simple, language-independent format. This step bridges the gap between conceptual design and implementation, ensuring clarity and consistency. Example pseudocode for a compressor stage could involve:

- Calculate outlet pressure using pressure ratio.
- Compute outlet temperature with isentropic efficiency.
- Determine work done based on temperature difference.

Step 7: Implement the Algorithm
Translate the pseudocode into a programming language. Choose a language suitable for the problem domain, such as MATLAB for numerical simulations or Python for general-purpose tasks. For the HPGTE simulation, implement the modules as MATLAB functions.

Step 8: Test the Algorithm
Run test cases to validate the algorithm against known results or theoretical expectations. Include edge cases, such as extreme efficiency values or pressure ratios, to ensure robustness. For example, verify that the turbine stage produces realistic temperature and pressure outputs under various conditions.

Step 9: Optimize the Algorithm
Refine the algorithm to improve performance, scalability, and accuracy. Optimize computational efficiency by reducing unnecessary calculations or using more efficient data structures. For example, streamline iterative calculations in the HPGTE simulation to reduce execution time.

Step 10: Document the Algorithm
Create detailed documentation for the algorithm, including its purpose, inputs, outputs, and step-by-step logic. This ensures that future users can understand, use, and maintain the algorithm effectively. For the HPGTE simulation, include comments in the code and a user guide for the GUI interface.

4. RESULT AND ANALYSIS

This Section focuses on the development and implementation of predictive computational models for failure analysis in turbine blades, emphasizing their mechanical behaviour under high-performance conditions. Using MATLAB, the study leverages thermodynamic principles and computational techniques to simulate the operational parameters of a High-Pressure Gas Turbine Engine (HPGTE). The implementation involves modelling critical components and processes such as compression, combustion, and turbine operations, ensuring accurate predictions of failure points and efficiency trends.

4.1 Computational Model Development

The computational framework is based on a modular design, where each engine component is modelled independently. The MATLAB GUI, developed using GUIDE, serves as an interactive tool for simulating engine behaviour. The following sections describe the individual modules:

Compressor Model: The Compressor Function calculates the outlet pressure, temperature, and work done by the compressor using the isentropic efficiency formula and conservation of energy principles. Inputs include the pressure ratio, efficiency, and inlet temperature.

Combustor Model: The Combustor Function incorporates heat addition and pressure loss in the combustion process. It calculates outlet conditions based on the mass flow rate of fuel, boiler worth, and combustion efficiency. This function is critical for determining turbine inlet conditions.

Turbine Model: The Turbine Function simulates energy extraction by calculating the temperature drop and outlet pressure using isentropic and mechanical efficiency factors. It also ensures mass flow continuity and computes the turbine's contribution to the overall work.

Exhaust Model: The Exhaust Function models the final stage, calculating outlet parameters and ensuring proper energy utilization. It determines the exhaust velocity and its contribution to thrust.

4.2 Implementation in MATLAB

The implementation involves translating the mathematical models into MATLAB functions and integrating them into a user-friendly GUI. The GUI allows for parameter inputs such as gas constants, specific heat capacities, pressure ratios, and efficiencies. Users can run simulations and view results in real-time through graphical plots.

Validation and Testing

Validation of the computational model is achieved by comparation simulation consequences with theoretical calculations and new data. For instance, temperature and pressure outputs from the combustor and turbine stages are cross-referenced with industry benchmarks. Additionally,

sensitivity analyses are conducted to identify critical parameters influencing turbine blade performance.

Design of GUI panel

The GUI designed in MATLAB-based simulation interface for a High-Pressure Gas Turbine Engine (HPGTE). It allows for the modelling and analysis of turbine behaviour by integrating thermodynamic principles into a user-friendly platform. The title emphasizes the development of predictive computational models for failure analysis in turbine blades, with a focus on mechanical behaviour under high-performance conditions.

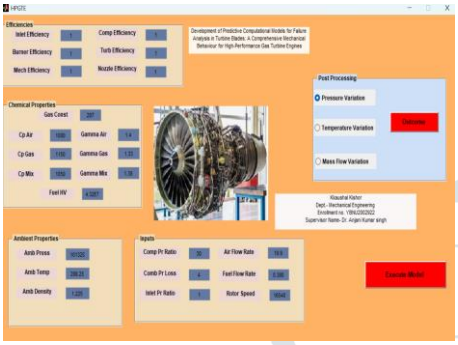

Fig. 2. Design of GUI panel

Key components of the GUI include

Efficiencies Section: Allows input for efficiency parameters of individual components, including inlet, compressor, burner, turbine, mechanical, and nozzle efficiencies.

Chemical Properties: Provides input fields for thermodynamic properties such as gas constant, specific heat capacities (Cp Air, Cp Gas, Cp Mix), and gamma values.

Ambient Properties: Inputs for ambient pressure, temperature, and density.

Engine Inputs: Parameters like pressure ratios, air and fuel flow rates, and rotor speed.

Post-Processing Options: Enables graphical visualization of variations in pressure, temperature, or mass flow across engine stages.

The GUI integrates visual elements, input validation, and an "Execute Model" button to simulate the engine and analyse results interactively, facilitating real-time insights into turbine behaviour and failure analysis.

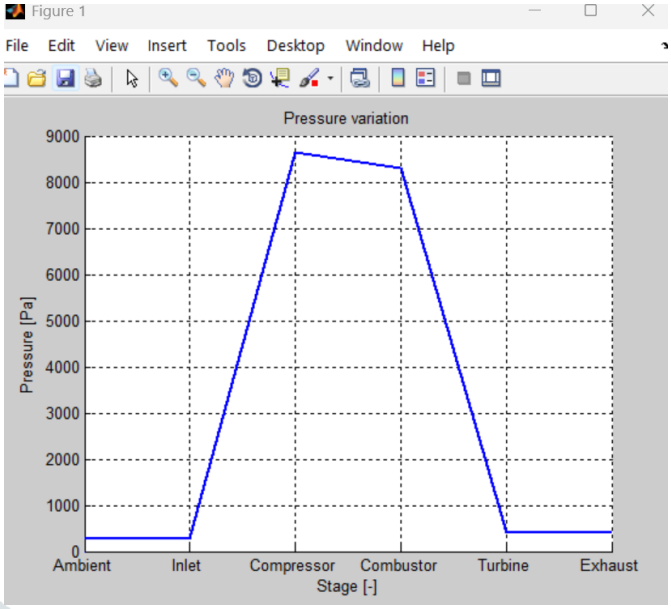

Fig. 3. Pressure Variation

The graph displayed represents the pressure variation across different stages of a High-Pressure Gas Turbine Engine (HPGTE) as generated by the MATLAB simulation. It provides a clear visual representation of the pressure changes occurring at various engine stages, including ambient, inlet, compressor, combustor, turbine, and exhaust.

Key Observations:

- Ambient to Inlet: The pressure remains nearly constant, reflecting the minimal pressure change in the inlet stage.
- Inlet to Compressor: A steep increase in pressure occurs, illustrating the primary role of the compressor in significantly boosting the pressure to support efficient combustion.
- Compressor to Combustor: The pressure is maintained at a high level, with minimal losses accounted for by the combustor pressure loss factor.
- Combustor to Turbine: A noticeable pressure drop occurs due to the energy extracted by the turbine to perform mechanical work and drive the compressor.
- Turbine to Exhaust: The pressure sharply decreases and stabilizes as gases expand into the atmosphere.

This graph effectively visualizes the impact of each component on pressure distribution, aiding in analysing engine performance and identifying potential areas for optimization. Such visualizations enhance the understanding of thermodynamic processes in turbine systems, supporting failure analysis and design improvements.

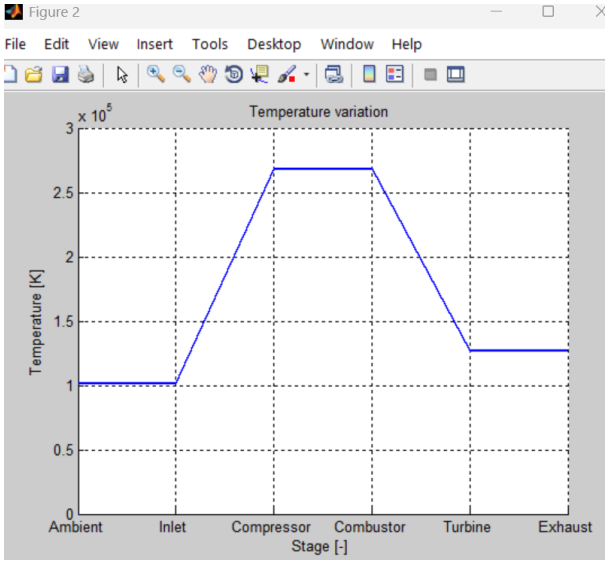

Fig. 4. Temperature Variation

The graph represents the temperature variation across the stages of a High-Pressure Gas Turbine Engine (HPGTE), generated by the MATLAB simulation. This visualization provides insights into how temperature changes as air and gases flow through the engine components.

Key Observations:

- Ambient to Inlet: The temperature remains relatively constant, reflecting the ambient conditions at the start of the process.
- Inlet to Compressor: A sharp increase in temperature is observed due to the work done by the compressor on the air, raising its thermal energy.
- Compressor to Combustor: The temperature reaches its peak in the combustor, where heat is added through fuel combustion. This high temperature is necessary for the turbine to extract maximum energy.
- Combustor to Turbine: A significant temperature drop occurs as the turbine excerpts liveliness from the high-temperature airs to drive the compressor and other mechanical components.
- Turbine to Exhaust: The temperature stabilizes at a lower value as the exhaust gases expand and release residual heat into the atmosphere.

This graph effectively illustrates the thermal dynamics of the engine, showing how each stage influences temperature. Such analysis is crucial for evaluating performance, ensuring optimal operation, and identifying potential failure points due to thermal stress.

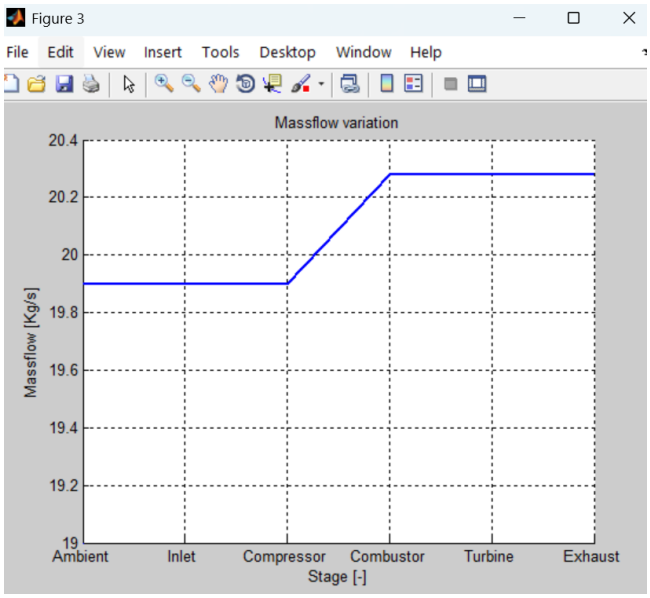

Fig. 5. Massflow Variation

The graph depicts the mass flow variation across the stages of a High-Pressure Gas Turbine Engine (HPGTE), generated from the MATLAB simulation. This analysis helps to understand how mass flow rates change throughout the engine stages.

Key Observations:

- Ambient to Inlet: The mass flow remains constant, representing the intake of air from the ambient environment without any significant changes.
- Inlet to Compressor: There is no noticeable alteration in the mass flow rate, as the compressor primarily compresses the air without altering its mass.
- Compressor to Combustor: A slight upsurge in mass flow rate occurs at the combustor stage. This is due to the addition of fuel mass to the compressed air for combustion.
- Combustor to Turbine: The mass flow remains constant after the combustor as the fuel-air mixture flows through the turbine. No additional mass is introduced during this stage.
- Turbine to Exhaust: The mass flow rate remains unchanged as the exhaust gases are expelled into the atmosphere.

This graph demonstrates the conservation of mass throughout the engine stages, with minor variations introduced by the addition of fuel during combustion. Such visualization is crucial for verifying the integrity of the mass balance in engine modelling and understanding operational dynamics.

4.3 Random Test Conditions and Outcome Visualization

To enhance the robustness of the blade design and analysis, the study incorporates the generation of **10 random test conditions** within realistic parameter ranges specific to high-performance gas turbines. This stochastic approach allows for the assessment of blade performance under varying operational scenarios, providing insights

into design sensitivity, performance variability, and potential failure modes.

Random Test Condition Generation: Limits such as the number of blades, rotor range, hub range, air density, design gas speed, and TSR are randomized within predefined ranges. For example, the number of blades varies between 2 and 10, rotor radius between 30 and 100 meters, and TSR between 5 and 10. This variability simulates a wide array of possible design configurations and operational conditions encountered in different high-performance gas turbine applications.

Outcome Computation: For each set of random inputs, the chord and twist distributions are recalculated, and power outputs are estimated using the same methodologies as the base model. Additionally, structural stress analysis is performed to estimate bending moments and stresses within the blade material, critical for failure analysis. These results are compiled into a MATLAB table, enabling easy comparison and analysis across different test cases.

Visualization Through Line Graphs: Line graphs are employed to visualize the relationships between various design parameters and power outputs, as well as structural stresses. Key visualizations include:

- **Power Comparison Line Graph:** Plots both ideal power (based on Cp = 0.45) and Betz limit power (Cp = 16/27) against the test case number, highlighting the efficiency range.
- **Power vs. TSR:** Illustrates how power outputs vary with TSR, providing insights into aerodynamic efficiency optimization.
- **Power vs. Design Gas Speed:** Shows the dependency of power generation on gas speed, emphasizing the association amid gas velocity and power production.
- **Power vs. Rotor Radius:** Demonstrates the association amid rotor size and control output, underscoring the importance of rotor dimensions in energy capture.
- **Bending Stress Distribution:** Visualizes the stress induced lengthways the knife-edge span, critical for identifying potential failure points.
- **Fatigue Life Distribution:** Depicts the estimated number of cycles each blade segment can endure before failure, highlighting segments that fall below the operational life.

These visualizations are instrumental in identifying trends, optimal parameter ranges, and potential areas for design improvement, ensuring that turbine blades are both aerodynamically efficient and mechanically robust.

4.4 Predictive Computational Models for Failure Analysis

Ensuring the **mechanical integrity and longevity** of turbine blades in high-performance gas turbine engines is paramount. The **predictive computational models** developed in this study integrate **aerodynamic force calculations**, **structural stress analysis**, and **fatigue life estimations** to provide a comprehensive framework for **failure analysis**. This integration is essential for identifying potential failure modes, estimating the blade's fatigue life, and optimizing the design to prevent catastrophic failures that could compromise engine performance and safety.

Model Components:

- **Aerodynamic Force Calculation:** The model calculates the lift and slog militaries acting on each knife-edge segment based on aerodynamic coefficients, gas speed, and blade geometry. These forces are fundamental in determining the resulting bending moments that induce stress within the blade material.
- **Bending Moment Calculation:** Accumulated lift forces along the blade span generate bending moments, which are calculated iteratively for each radial segment. The bending moment is a key determinant of induced stress in the blade material, especially under high-pressure, high-temperature gas conditions prevalent in gas turbines.
- **Stress Analysis:** Using the bending moments, the model computes the induced bending stress at each segment. The stress is calculated assuming a simplified rectangular cross-section, considering both the chord length and the moment of inertia. This simplification allows for rapid assessment of stress distributions without delving into complex geometries, though it may overlook nuanced stress concentrations in actual blade profiles.
- **Fatigue Life Estimation:** Employing Basquin's equation, the model estimates the fatigue life of each blade segment. This estimation compares the induced stress against the material's endurance limit, adjusted for a care issue; to predict the number of series a segment can withstand before failure. Fatigue life is a critical metric, as turbine blades undergo millions of operational cycles under varying loads and temperatures.

Assumptions and Simplifications:

- **Material Homogeneity:** The model assumes uniform material properties across the blade span, which may not account for real-world variations due to manufacturing processes, material defects, or localized cooling treatments.
- **Static Loading:** Only bending stresses are considered, neglecting torsional and axial stresses that can also contribute to blade fatigue and failure under dynamic gas flows.
- **Simplified Fatigue Model:** Basquin's equation provides a basic S-N curve-based fatigue life estimation, suitable for preliminary analysis but potentially oversimplifying complex fatigue behaviours influenced by multiaxial stresses and high-temperature effects.

Results and Failure Prediction: The model identifies blade segments that are at risk of failure by comparing the

estimated fatigue life against the expected operational life (e.g., 10 million cycles). Segments with fatigue life below this threshold are flagged, indicating potential failure points that require design intervention or material reinforcement. This predictive capability is crucial for proactive maintenance scheduling, design optimization, and safeguarding the safe process of gas turbine trains.

Visualization of Failure Analysis: Several plots are generated to visualize the failure analysis results:

- **Bending Stress Distribution:** Shows the variation of induced bending stress along the blade span, with a reference line indicating the yield stress adjusted by the safety factor. This plot helps identify regions of high stress that may be prone to yielding or fatigue.
- **Fatigue Life Distribution:** Depicts the estimated number of cycles each blade segment can endure before failure, highlighting segments that fall below the operational life. This visualization aids in pinpointing critical areas requiring design optimization.
- **Failed Segments Highlighted:** An optional plot emphasizes the specific blade segments predicted to fail, facilitating targeted design improvements and material selection to enhance blade reliability.

These visualizations provide a clear and intuitive understanding of the structural performance and potential failure points within the blade design, enabling engineers to make informed decisions to mitigate risks.

4.5 Customized Designed for Turbine

Table 1. Test Conditions and Outcomes

B	R (m)	r_h (m)	rho (kg/m³)	V_design (m/s)	TSR	PowerIdeal_kW	PowerBetz_kW
5	60.055	2.2742	1.2808	11.233	5.4753	2742.9	3620.3
9	83.483	2.1763	1.2818	7.6899	8.5990	1805.8	2383.8
3	38.511	1.0594	1.2564	8.6512	7.0812	765.0	999.1
6	76.080	1.7367	1.2301	11.558	6.2504	3146.8	4158.2
7	72.975	1.5374	1.2760	8.1199	8.2300	1660.5	2190.9
6	49.091	2.8865	1.2493	10.858	9.5596	2244.2	2961.8
8	66.015	2.8399	1.2731	11.276	7.9290	2869.3	3789.4
8	72.591	2.2353	1.2672	11.008	5.0245	2595.3	3422.5
2	94.005	2.2167	1.2751	11.107	9.1520	5044.7	6659.2
3	43.555	2.0142	1.2722	6.1919	5.5027	360.5	475.6

Column Descriptions

B: Number of Blades
The total count of blades attached to the turbine rotor.
R (m): Rotor Radius
The radius of the turbine rotor in meters.
r_h (m): Hub Radius
The radius from the centre of the blade to the hub where edges are attached, in meters.
rho (kg/m³): Air Density
The thickness of air, characteristically round 1.225 kg/m³ at sea level. Variations can occur based on altitude and temperature.
V_design (m/s): Design Wind Speed
The wind haste at which the turbine is optimized to operate, measured in meters per second.

TSR: Tip-Speed Ratio
The ratio that compares the speed of a wind turbine's blade tip to the speed of the wind is known as the tip speed ratio (TSR). This value is crucial in determining the efficiency of a wind turbine, as it directly impacts its ability to convert wind energy into rotational energy.
PowerIdeal_kW: Estimated Power (Cp=0.45)
The estimated electrical power output in kilowatts based on an assumed power coefficient (Cp) of 0.45, which is typical for good turbine designs.
PowerBetz_kW: Betz-Limit Power
The theoretic all-out control that can be removed from the wind, based on the Betz boundary (Cp=16/ 27≈0.593)
Betz Limit: The Betz limit represents the maximum possible Cp for a wind turbine, which is approximately 59.3%. Practical turbines achieve lower Cp values due to various inefficiencies.

4.8 Test Conditions and Outcomes

This research conducts the test conditions and outcomes for a customized turbine design. The dataset contains key parameters such as blade count (B), blade radius (R), hub radius (r_h), air density (ρ), design velocity (V_design), Tip-Speed Ratio (TSR), and power outputs (PowerIdeal_kW and PowerBetz_kW). The analysis focuses on understanding the relationships between these parameters and turbine performance under varying conditions.

Overview of Key Parameters

Blade Count (B): The number of knife-edges straight influences the aerodynamic presentation and efficiency of the turbine. Higher blade counts typically enhance torque but may reduce rotational speed.
Blade Radius (R): The overall radius of the turbine affects the swept area and potential energy capture.
Hub Radius (r_h): The hub size determines the effective blade length, which influences the aerodynamic efficiency.

Air Density (ρ): Air density directly affects the kinetic energy available for conversion to mechanical power. Variations in ρ impact the overall power output.
Design Velocity (V_design): The velocity of incoming wind or fluid at which the turbine is optimized to perform.
Tip-Speed Ratio (TSR): The relation of the tip haste of the blades to the breeze velocity. TSR is critical in defining the efficiency and aerodynamic behavior of the turbine.

- **Power Outputs (PowerIdeal_kW and PowerBetz_kW):** These represent the ideal power and the theoretical maximum power achievable according to Betz's limit, respectively.

Data Interpretation

The test outcomes provide insights into turbine performance under different conditions. The following analysis examines the relationships and trends across the parameters.

Blade Count (B): Blade count values range from 2 to 9. A lower blade count (e.g., B=2 or 3) results in lower torque and higher rotational speeds, ideal for high TSR values. For example, in the test condition with B=2, the TSR reaches 9.1520, and the turbine achieves the highest power outputs (PowerIdeal_kW = 5044.7, PowerBetz_kW = 6659.2). Conversely, higher blade counts (e.g., B=8 or 9) provide increased torque and better performance at lower TSR values. For instance, with B=9, the TSR is 8.5990, and the turbine achieves substantial power outputs (PowerIdeal_kW = 1805.8, PowerBetz_kW = 2383.8).

Blade Radius (R): The blade radius ranges from 38.511 m to 94.005 m. Larger radii (e.g., R=94.005) increase the swept area, capturing more energy from the wind and improving power output. This is evident in the case with R=94.005 m, where the turbine achieves the highest power values. Smaller radii (e.g., R=38.511) result in a reduced swept area and lower power outputs. This is observed with PowerIdeal_kW = 765.0 and PowerBetz_kW = 999.1 at R=38.511 m.

Hub Radius (r_h): The hub radius values range between 1.0594 m and 2.8865 m. A smaller hub radius allows for longer blades, increasing the effective swept area. For example, with r_h = 1.0594 m and R = 38.511 m, the turbine achieves moderate power outputs (PowerIdeal_kW = 765.0). Larger hub radii reduce the effective blade length, impacting efficiency. In the case with r_h = 2.8865 m, PowerIdeal_kW is 2244.2, which is lower than turbines with similar R but smaller r_h values.

Air Density (ρ): Air density remains relatively constant across tests, ranging from 1.2301 kg/m³ to 1.2818 kg/m³. This slight variation is typical of different atmospheric conditions but has a proportional effect on power output. For example, when ρ increases from 1.2301 kg/m³ to 1.2818 kg/m³, corresponding power outputs increase slightly.

Design Velocity (V_design): Design velocity values range from 6.1919 m/s to 11.558 m/s. Higher velocities significantly enhance power output due to the cubic relationship between velocity and kinetic energy. For instance, with V_design = 11.558 m/s, PowerIdeal_kW = 3146.8 and PowerBetz_kW = 4158.2, representing high energy capture efficiency. Lower velocities, such as V_design = 6.1919 m/s, yield reduced power outputs, with PowerIdeal_kW = 360.5 and PowerBetz_kW = 475.6.

Tip-Speed Ratio (TSR): TSR values vary from 5.0245 to 9.5596. An optimal TSR ensures maximum aerodynamic efficiency. Higher TSRs, such as 9.1520, result in higher power outputs, as seen with B=2. Conversely, lower TSRs, such as 5.0245, correlate with moderate power outputs (PowerIdeal_kW = 2595.3).

Power Outputs (PowerIdeal_kW and PowerBetz_kW): PowerIdeal_kW represents the practical power achieved under ideal conditions, while PowerBetz_kW reflects the theoretical limit. The ratio of these values provides insights into the turbine's efficiency. The highest PowerIdeal_kW value (5044.7) occurs with B=2, R=94.005, and TSR=9.1520, demonstrating optimal energy capture. Lower PowerIdeal_kW values, such as 360.5, correspond to less favourable conditions, including low R and V_design values.

5. CONCLUSION, FINDINGS AND FUTURE SCOPE

The dataset delivers valued visions into the presentation of customized turbine designs under various conditions. Key limits such as knife-edge count, radius, design speed, and TSR significantly influence power output. Optimizing these factors in synergy can maximize efficiency and energy capture. This analysis highlights that the most efficient performance is achieved when blade count, radius, and TSR align with high design velocities and minimal hub radius.

Findings

The findings from the analysis reveal that turbines with a low blade count (e.g., B=2 or 3) and a high blade radius (e.g., R=94.005 m) perform exceptionally well, particularly when coupled with high design velocities and optimized TSR. Smaller hub radii further enhance performance, as they maximize the effective blade length and energy capture area. Additionally, the results confirm the significant impact of design velocity on power output, underscoring the importance of location-specific optimization to match environmental wind speeds. The theoretical maximum efficiency, as described by Betz's law, serves as a benchmark, with practical outputs closely approximating this limit under ideal conditions.

Future Scope

The study delivers a basis for additional examination and innovation in turbine project. Future research can investigate:

- **Blade Material Optimization:** Exploring advanced materials for improved strength-to-weight ratios and aerodynamic efficiency.
- **Dynamic Blade Pitching:** Implementing adaptive blade angles to maintain optimal TSR under varying wind conditions.

- **Real-Time Monitoring:** Integrating IoT devices for real-time performance tracking and predictive maintenance.
- **Aerodynamic Enhancements:** Designing blade geometries to reduce drag and turbulence.
- **Environmental Adaptation:** Analysing performance under extreme conditions, such as high-altitude or offshore environments.

Reference

1. Frunzăverde, D., Muntean, S., Mărginean, G., Campian, V., Marşavina, L., Terzi, R., & Şerban, V. (2010, August). Failure analysis of a Francis turbine runner. In *IOP conference series: earth and environmental science* (Vol. 12, No. 1, p. 012115). IOP Publishing.
2. Silveira, E., Atxaga, G., & Irisarri, A. M. (2010). Failure analysis of two sets of aircraft blades. *Engineering Failure Analysis*, *17*(3), 641-647.
3. Choi, Y. S., & Lee, K. H. (2010). Investigation of blade failure in a gas turbine. *Journal of mechanical science and technology*, *24*, 1969-1974
4. Sujata, M., Madan, M., Raghavendra, K., Venkataswamy, M. A., & Bhaumik, S. K. (2010). Identification of failure mechanisms in nickel base superalloy turbine blades through microstructural study. *Engineering Failure Analysis*, *17*(6), 1436-1446.
5. Shankar, M., Kumar, K., & Prasad, S. A. (2010). T-root blades in a steam turbine rotor: A case study. *Engineering Failure Analysis*, *17*(5), 1205-1212.
6. Barella, S., Boniardi, M., Cincera, S. I. L. V. I. A., Pellin, P., Degive, X., & Gijbels, S. (2011). Failure analysis of a third stage gas turbine blade. *Engineering Failure Analysis*, *18*(1), 386-393.
7. Chen, C. P., & Kam, T. Y. (2011). Failure analysis of small composite sandwich turbine blade subjected to extreme wind load. *Procedia Engineering*, *14*, 1973-1981.
8. Kargarnejad, S., & Djavanroodi, F. (2012). Failure assessment of Nimonic 80A gas turbine blade. *Engineering Failure Analysis*, *26*, 211-219.
9. Lee, Y. J., Jhan, Y. T., & Chung, C. H. (2012). Fluid–structure interaction of FRP wind turbine blades under aerodynamic effect. *Composites Part B: Engineering*, *43*(5), 2180-2191.
10. Qu, S., Fu, C. M., Dong, C., Tian, J. F., & Zhang, Z. F. (2013). Failure analysis of the 1st stage blades in gas turbine engine. *Engineering Failure Analysis*, *32*, 292-303.
11. Poursaeidi, E., Babaei, A., Behrouzshad, F., & Arhani, M. M. (2013). Failure analysis of an axial compressor first row rotating blades. *Engineering Failure Analysis*, *28*, 25-33.
12. Yang, B., & Sun, D. (2013). Testing, inspecting and monitoring technologies for wind turbine blades: A survey. *Renewable and Sustainable Energy Reviews*, *22*, 515-526.
13. Rao, V. N. B., Kumar, I. N., & Prasad, K. B. (2014). Failure analysis of gas turbine blades in a gas turbine engine used for marine applications. *International Journal of Engineering, Science and Technology*, *6*(1), 43-48.
14. Khawaja, H., & Moatamedi, M. (2014). Selection of high performance alloy for gas turbine blade using multiphysics analysis. *The International Journal of Multiphysics*, *8*(1), 91-100.
15. Zhao, R., Zhuge, W., Zhang, Y., Yang, M., Martinez-Botas, R., & Yin, Y. (2015). Study of two-stage turbine characteristic and its influence on turbo-compound engine performance. *Energy Conversion and Management*, *95*, 414-423.
16. Clarkson, R. J., Majewicz, E. J., & Mack, P. (2016). A re-evaluation of the 2010 quantitative understanding of the effects volcanic ash has on gas turbine engines. *Proceedings of the Institution of Mechanical Engineers, Part G: Journal of Aerospace Engineering*, *230*(12), 2274-2291.
17. Adamou, A., Costall, A., Turner, J. W., Jones, A., & Copeland, C. (2023). Experimental performance and emissions of additively manufactured high-temperature combustion chambers for micro-gas turbines. *International Journal of Engine Research*, *24*(4), 1273-1289.
18. Alnaeli, M., Alnajideen, M., Navaratne, R., Shi, H., Czyzewski, P., Wang, P., ... & Bowen, P. J. (2023). High-temperature materials for complex components in ammonia/hydrogen gas turbines: a critical review. *Energies*, *16*(19), 6973.
19. Hong, C. W., & Kim, J. (2023). Exhaust temperature prediction for gas turbine performance estimation by using deep learning. *Journal of Electrical Engineering & Technology*, *18*(4), 3117-3125.
20. Zhang, X., Zhong, M., Ooi, K. T., & Zhang, T. (2024). Incipient instability real-time warning via adaptive wavelet synchrosqueezed transform: Onboard applications from compressors to gas turbine engines. *Energy*, *308*, 132925.
21. Jin, Y., Huang, Y., Yao, K., Zhang, K., Wang, Y., & Wang, D. (2024). Ignition and Lean Blowout Characteristics of a Reverse-Flow Combustor for an Ultra-Compact Gas Turbine Engine. *Journal of Thermal Science*, *33*(5), 1897-1906.
22. Asaad, W., Shaker, L. M., & Kdhim, R. H. (2024). Overview of a Gas Turbine Blades Power Plant. *Al-Salam Journal for Engineering and Technology*, *3*(1), 117-127.
23. Enyia, D. J., Ansa, U. E., Osim-Asu, D., Ogochukwu, C. J., & Enyia, S. J. D. (2024). Performance Improvement of Industrial Gas Turbine for Power Augmentation in the Nigeria Oil and Gas Sector. *International Journal of Innovative Research in Engineering and Management*, *11*(4), 67-80.
24. Feiz, H., Karim, H., Mitchell, M., Song, J., Kubicki, D., Kumar, V., ... & Lee, J. G. (2024). Evaporation Modeling of Multiple Liquid Jets in Crossflow Used in Gas Turbine Injector Development. In *AIAA SCITECH 2024 Forum* (p. 1998).